INFLUENCE OF CHEMICAL PURITY ON THE PROPAGATION OF FATIGUE CRACKS IN Al-Zn-Mg-Cu ALLOYS

G. Chalant*

Two 7075 type Aluminum alloys with different Fe and Si content are compared. Low cycle fatigue properties are found to be nearly the same. Fatigue crack propagation rates are lowered in the high purity alloy. This effect is explained in terms of crack closure at low rates and fracture toughness at high rates. Closure is shown to be roughness dependent.

INTRODUCTION

Increasing fatigue and fracture resistance of Aluminum alloys currently used in aeronautic industry is one of the major goals to achieve higher security, low-cost maintenance, and increased payload. Research has been initiated in two directions:

- finding better thermomechanical treatments for existing alloys, with increasing knowledge of chemical and microstructural evolution and their effect on mechanical characteristics of the material
- finding new materials through evoluation of chemical composition of current material (2xxx and 7xxx series) or with brand-new materials (such as Al-Li-Cu alloys).

Changing the impurity level of 7075 type alloys has not been that much investigated (1) to (7), and it is quite hard to make its own opinion on all mechanical characteristics (then on commercial potential use) using the open literature,

* Laboratoire de Mécanique et de Physique des Matériaux.
UA CNRS 863 - E.N.S.M.A. 86034 POITIERS Cedex - FRANCE

The purpose of this investigation (which is at its beginning) is to deal with crack propagation under fatigue conditions, from both physical and mechanical point of view.

In this paper, considerations are directed to evaluation of two 7075 type alloys with differences in Fe and Si content.

Monotonic properties are presented and low cycle fatigue behaviour is compared with respect to mechanical properties (namely cyclic stress-strain curve).

Fatigue crack propagation is investigated for one loading ratio in the medium rate range and differences are shown to depend on the purity level.

Using closure analysis, evaluated by means of the commonly used compliance technique, mechanisms of fatigue crack growth are evaluated and a transition regime between active mechanisms is pointed out.

Then closure itself, which is shown to differ in both cases, is explained in term of roughness-induced closure phenomenon, and secondary cracking which occur only in the high purity alloy.

EXPERIMENTAL

A - Materials

Two different aluminum alloys based on 7075 composition are used in this study. In order to investigate in both alloys the purity level effect different Fe and Si contents are checked. Lowering the Fe and Si content leads to less intermetallic particles Al7 Cu2 Fe and Mg2 Si which are of major importance to fracture toughness (2-4) and fatigue crack initiation (5, 8, 9). The amount of those large particles (1 to 20 µm) is higher in the commercial grade alloy 7075 than in the high purity alloy 7X75. Compositions, in weight percent, of both alloys are given in table 1.

TABLE 1 - Chemical compositions.

Alloys	Zn	Mg	Cu	Cr	Ti	Mn	Fe	Si	Fe+Si
7075	5.80	2.35	1.51	0.21	0.05	0.04	0.17	0.08	0.25
7X75	5.93	2.09	1.49	0.19	0.02	0.02	0.02	0.03	0.05

Both alloys are given with conventional T7351 thermomechanical treatment: solution heat treated at 465 °C, water quenched, 1.5 to 3% controlled stretching, followed by a two stages heat treatment of 6 to 8 hours at 108 °C and 24 to 30 hours at 161 °C.

This thermomechanical treatment is currently encountered in aeronautical structures for it gives a good balance between mechanical properties in tension and fatigue, fracture toughness and corrosion resistance. The mechanical properties are summarized in table 2 and noteworthy is the improvement of fracture toughness (by a factor of 2 in all directions) for the high purity alloy as compared to the commercial grade one. On the other hand the elastic 0.2% proof stress and ultimate tensile stress are very close for both alloys and almost equal in all three directions, (respectively σ_E = 400 MPa, σ_R = 482 MPa for 7075, and σ_E = 388 MPa, σ_R = 470 MPa for 7X75).

Due to a lower amount of intermetallic hard particles, the permanent elongation after failure in tension is larger in the high purity alloy in all three directions. A difference is observed in the short transverse direction (5.6% for 7075 as compared to 11.8% for 7X75) see table 2.

TABLE 2 - Mechanical properties.

Alloys	K_{Ic} MPa $\sqrt{m}$	σ_E 0,2% MPa	σ_R MPa	Elongation A%	Orientation
7075	41.2	398	481	13.5	LT
	32.0	408	492	10	TL
	25.7	394	472	5.6	SL
7X75	76.9	390	464	16	LT
	59.9	395	474	13.4	TL
	53.5	380	470	11.8	SL

From the microstructural point of view, thermomechanical treatment leads to a pancake like grain structure.

For the commercial grade alloy 7075, the grain size is 500 µm in the rolling direction, 200 µm in the transverse direction and 20 µm in the short transverse direction.

For the high purity alloy 7X75, the grain size is 8000 µm in the rolling direction, 350 µm in the transverse direction and 310 µm in the short transverse direction.

Both materials have been received in rolled sheets form (about 70 mm) and exhibit some variations in grain size due to differences in volume fraction of intermetallic particles.

B - Low cycle fatigue (LCF) experiments

Low cycle fatigue tests were performed on a closed loop servo-hydraulic testing machine, under push-pull tension compression conditions with a strain ratio R = -1. Cylindrical specimens tested under plastic axial strain control were used in order to compare the cyclic stress-strain responses of both materials, and fatigue life Manson-Coffin curves as well. Tests were conducted at room temperature (about 24 °C), under air atmosphere with room relative humidity (about 55%). During the tests, the average total deformation rate was kept constant (3 to $5 \cdot 10^{-3}$ s^{-1}).

The load variation was continuously monitored on a X-time strip chart recorder, and hysteresis stress-strain loops were periodically recorded at logarithmic intervals.

The axisymmetric low cycle fatigue specimens, were machined with the TL orientation (cracks initiate and propagate in the rolling direction), with an active cylindrical gage of 8 mm in diameter.

C - Fatigue crack propagation (FCP) experiments

FCP experiments were carried out on a closed loop servo-hydraulic testing machine, with the same environmental conditions as for LCF experiments (air, 24 °C, 55% RH). FCP specimens are Compact Tension (CT) specimen with a width W = 75 mm and a thickness B = 10 mm. Since only the mid-range of stress intensity factor (ΔK = 7 to 30 MPa $\sqrt{m}$) was intended to be explored to establish the stage II Fatigue Crack Growth Rate (FCGR) curves, say da/dN versus ΔK (with da/dN 10^{-8} to 10^{-5} m/cycle), tests were conducted under constant load amplitude. A sine load wave, with frequency from 40 Hz to 10 Hz (for high FCGR), and a load ratio R = 0.1, was used.

During tests, the crack length (a) was measured using a travelling microscope (accuracy 10 μm). Then fatigue crack growth rates and stress intensity factors were calculated according to ASTM specifications (10).

D - Crack closure measurements

CT specimens were designed according to the ASTM standard (11) in order to measure compliance variation during the experiments. This technique is the most common one to ensure an accurate measurement of effective stress intensity factor (ΔK_{eff}) as defined by Elber (12). At a test frequency to 0.03 Hz the opening displacements (δ) and corresponding loads (P) were periodically recorded on a X-Y strip chart recorder. A more

accurate evaluation of ΔK_{eff} can be done using a "reduced" displacement (13) $\delta' = \alpha P-\delta$ where α is a constant, adjusted to be close to the compliance of the specimen. Those curves allow a good determination of the current compliance ($P-\delta$) and of effective stress intensity factor, ΔK_{eff} (cf. figure 1). The experiments have to be executed carefully because the technique is not free from artefacts.

E - Metallographic observations

In order to evaluate differences in physical crack propagation and crack closure mechanism crack paths on both sides of two specimens were observed by optical microscopy. Maps of micrographs were taken all along cracks from notch to crack tip ($a/W = 0.7$). In addition, crack path asperities (heights and angles) were measured (cf. figure 2).

Assuming differences in closure phenomena between both alloys to be only due to purity effects and not to mechanical or microstructural differential properties, crack path characteristics must account for clusure variations (see figure 2).

RESULTS AND DISCUSSIONS

A - Low cycle fatique (LCF)

In the LCF experiments the cyclic mechanical properties of the two alloys are determined. One can see (figure 3) that stress evolution during LCF tests is quite similar in both alloys. In fact the most striking feature is that there is no stress variation, neither hardening nor softening. This means that monotonic stress-strain curve (which can be drawn from the very first fatigue half cycle of each test) is very close to the cyclic stress-strain curve. As it can be seen from figure 4, there is no influence of purity level on cyclic mechanical properties. These results, (17), suggest that differences encountered in fatigue crack propagation should not be attributed to mechanical properties (6), (18).

In fact, in this case, the purity parameter influence is very well isolated and responsible for fatigue life variations (8), (18) crack initiation (8), (9) and fatigue crack propagation (7).

B - Fatigue crack propagation

Fatigue crack propagation tests were conducted with a load ratio $R = 0.1$, under air atmosphere (RH = 0.55%) at room temperature (24 °C). Results, in figure 5, show a systematic decrease (by a factor of 3) of FCGR in 7X75 high purity alloy as compared to the 7075 commercial alloy. This difference is quite

uniform in all the FCGR range in this investigation, say from 10^{-8} m/cycle to 10^{-5} m/cycle. Therefore reducing the impurity level gives rise to a significant reduction of crack propagation rate.

This feature is thought mainly due to two effects:

- the closure behaviour is different for both alloys (higher opening loads for 7X75 high purity alloy)
- the mechanisms of fatigue crack propagation are different in the high stress intensity factor region.

C - Crack closure and propagation mechanisms

The crack opening loads have been estimated using the common compliance technique as explained in part II D. In order to ensure accuracy of the measurements, fully opened specimen compliance was measured in the P-δ region where the crack is open. Those measurements have been cross-checked with calculations of the theoretical elastic compliance (19). The results of measurements and calculations which are in good agreement, cf. figure 6, give confidence for further examination.

Effective stress intensity factors (ΔK_{eff}) can be derived from these recordings and used into account for closure in fatigue crack propagation thus giving effective FCGR curves. It can be seen from figure 7, that:

- in the low FCG rate, da/dN, region the different behaviour of the two alloys, disclosed in figure 5 can be explained from differences in the closure behaviour
- in the high FCG rate region, transitional to stage III, there is almost no closure, and differences between 7075 and 7X75 increase with the stress intensity factor. This feature can be explained as a transition of crack propagation mechanisms (20), (21).

In the low da/dN region, crack propagates by fatigue damage accumulation at the crack tip (22). In the high da/dN region ductile rupture in the plastic zone becomes the more predominant fracture mechanism (2), (7). As shown in table 2, the fracture toughness differs by a factor of two, and the 7X75 high purity alloy can hold higher stress intensity factors.

D - Origin of differences in closure behaviour

Optical micrographs maps taken along crack path occurence along faces of specimens show evidence of differential fatigue cracking behaviour relative to impurity content (i.e. large second phase particles) in the 7075 type alloy. Figure 2, as well as

figures 8 and 9, illustrate the two most striking differences in crack path appearence. In 7X75 high purity alloy:

- profuse secondary cracking occurs, especially in the crack path region corresponding to low da/dN FCG rates for shorter crack length (remembering FCP test were conducted with ΔP constant load amplitude). This region correspond to the maximum differences in closure behaviour, say for ΔK under 13 MPa $\sqrt{m}$. It must be noticed that no secondary cracking occurs in the 7075 commercial purity alloy.

Roughness is comparatively higher. According to several authors, (24) to (27), crack closure loads vary with roughness. Several roughness-induced closure models have been tentatively established to account for higher closure in rough crack path materials, (24), (27), (28).

Roughness is caused by physical contact between crack surfces:

- either by local mixed mode displacement at the crack tip, (only mode I and II for some authors (27) to (29))
- or by plastic deformation of crack surfaces preventing complete geometic concordance of both sides, as supposed by some authors, (24), (30), (31).

For the case of purity influence, the investigation is in progress, but preliminary results shows that plastification should not be considered with respect to similar fatigue stress-strain behaviour, excepted if plastic deformation must be considered on both paths of branched cracks (for 7X75 alloy).

First measurements taken from micrographs (cf. figures 8 and 9) show that there are some higher asperities in the 7X75 high purity alloy as it can be seen on figures 10 and 11.

At least, as seen on figure 9, one must notice some holes at the crack branching of 7X75 alloy, which correspond to a lack of material isolated by secondary microcracks. This kind of debris may lead to a strong increase of closure level if they lie in between crack surfaces.

CONCLUSIONS

Decreasing the content of Fe and Si impurities leads to a decrease of the volume fraction of intermetallic large particles. Doing this, fracture toughness is strongly increased, but cyclic stress-strain response is similar.

Fatigue crack propagation rates is lowered in a high purity alloy as compared to a commercial purity one. These differences in behaviour have been shown to be due to two main causes:

- in the low FCG rate region (under 10^{-7} m/cycle), closure fully accounts for rates differences through effective stress intensity factor variation. The closure behaviour has been attributed to surface roughness and secondary cracking.
- in the high FCG rates region (above 10^{-6} m/cycle) propagation mechanism is toughness controlled for K_{max} approaches K_{Ic}.

ACKNOWLEDGEMENT

The author gratefully acknowledges D. Aliaga and the "Société Aérospatiale" for financial support, also B. Audubert and F. Delhaye for their help in FCP experiments.

REFERENCES

(1) Santner, J.S. and Eylon, D., Met. Trans., 10A, 1979, pp. 841-848.

(2) Van de Kasteele, J.C.W. and Broek, D., Eng. Fract. Mech., 9, 1977, pp. 625-635.

(3) Santner, J.S., Met. Trans., 9A, 1978, pp. 679-779.

(4) Lacroix, J.Y. and Mace, R., Mem. Sc. Rev. Met., 1985, pp. 213-221.

(5) Reimann, W.H. and Brisbane, A.W., Eng. Fract. Mech., 5, 1973, pp. 67-78.

(7) Albrecht, J. and Lutjering, G., Metal Science, 15, 1981, pp. 323-329.

(8) Starke, E.A. and Lutjering, G., in "Fatigue and microstructure" American Society for Metals Pub., 1979, pp. 205-243.

(9) Carre, C., Aerospatiale Report, MAT 290, Nb 44733/F, february 1985.

(10) ASTM Standard, E 647-83.

(11) ASTM Standard, E 813-81.

(12) Elber, W., Eng. Fract. Mech., 2, 1970, pp. 917-920.

(13) Kikukawa, M., J. of Mat. Sc. 26, 1977, p. 1964.

(14) Fuhring, H., Int. J. of Fracture, 12, 1976, pp. 917-920.

(15) James, M.N. and Knott, J.F., Mat, Sc. Engng., 72, 1985, pp. L1-L4.

(16) Lafarie-Frenot, M.C., Private communication.

(17) Chalant, G., Aerospatiale Report, Nb 50438356 ER/JB, Oct. 1985.

(18) Ferton, D., DGRST Report, Nb 77-7-0894, August 1979.

(19) Saxena, A. and Hudak, S.J., Int. J. of Fracture, 14, 1978, pp. 453-468.

(20) Clavel, M. and Pineau, A., Mat. Sc. and Engng., 55, 1982, pp. 173-180.

(21) Chalant, G., Thesis Doctorat d'Etat, University of Paris XI, Orsay Nb 2512, November 1981.

(22) Chalant, G. and Remy, L., Eng. Fract. Mech., 18, 1983., pp. 939-952.

(23) Walker, N. and Beevers, C.J., Fatigue of Eng. Mat. Struct., 1, 1979, pp. 135-148.

(24) Beevers, C.J., Bell, K., Carlson, R.L. and Starke, E.A., Eng. Fract. Mech., 19, 1984, pp. 93-100.

(25) Lafarie-Frenot, M.C. and Gasc, C., in "Advances in Fracture Research", ICF6, Pergamon Press, 1984, pp. 2041-2048.

(26) Vincent, J.N. and Remy, L., in "Fatigue 84", EMAS Pub. 1984, Vol. II, pp. 697-706.

(27) Bievers, C.J. and Carlson, R.L., ibid., Vol. II, pp. 655-665.

(28) Suresh, S. Met. Trans., 16A, 1985, pp. 249-260.

(29) Kwon, J.H., Ph. D. Thesis, University of Poitiers Nb 01, march 1985.

(30) Lafarie-Frenot, M.C., Thesis Doctorat d'Etat, University of Poitiers, march 1986.

(31) Purushothaman, S. and Tien, J.K., in "Strength of metals and alloys", ICSMA5, Pergamon Press, 1979, Vol. 2, pp. 1267-1271.

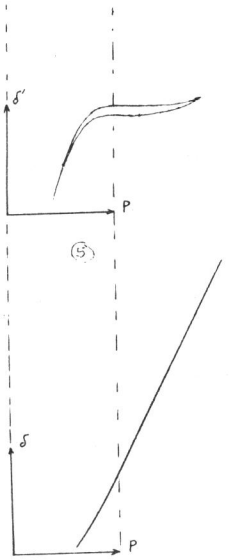

Figure 1 Typical example of compliance curves P-δ and P-δ' for for 7X75

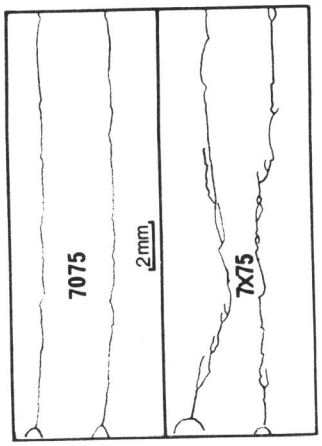

Figure 2 Path of fatigue crack for both alloys: 7075 and 7X75

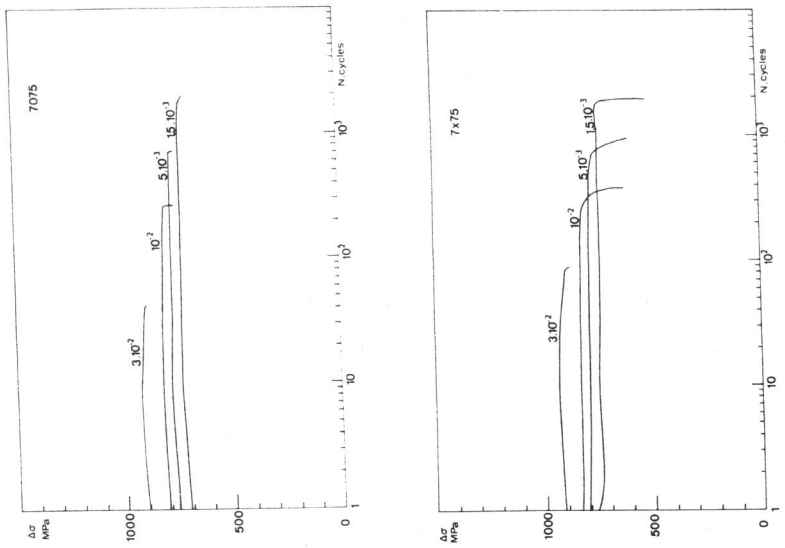

Figure 3 7075 and 7X75: Stress evolution for several low cycle fatigue tests

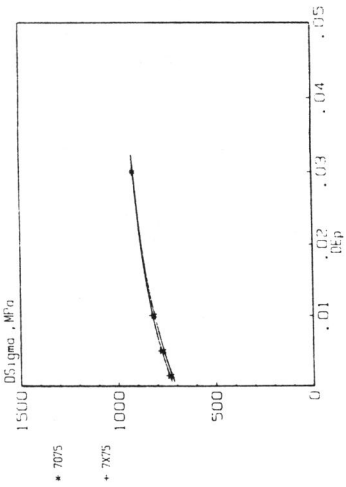

Figure 4 7075 and 7X75: cycle stress-strain curves comparison

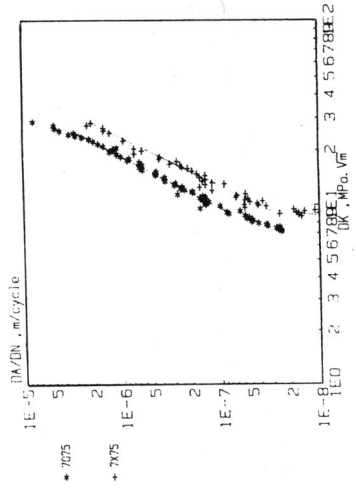

Figure 5 7075 and 7X75: comparison of fatigue crack growth rates (FCGR)

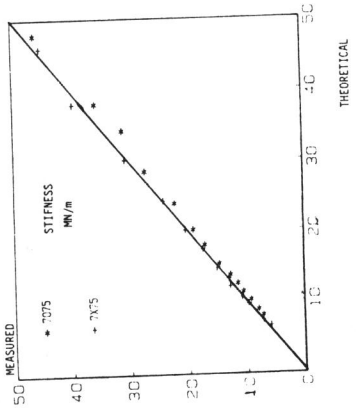

Figure 6 7075 and 7X75: measured vs calculated CT specimen stifness

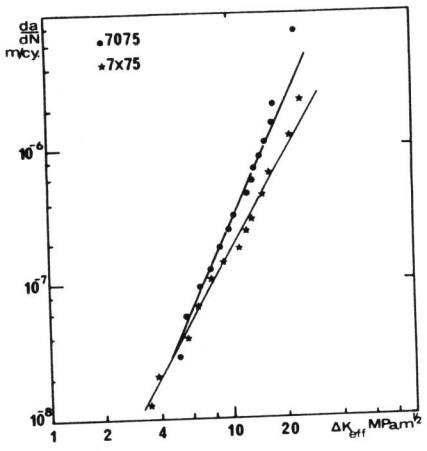

Figure 7 7075 and 7X75: comparison of effective FCGR curves

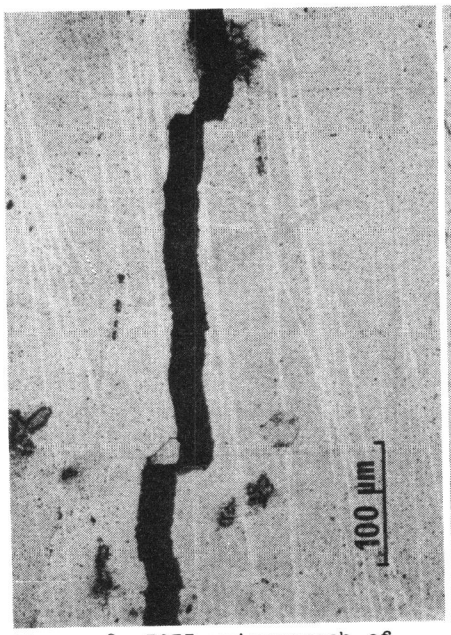

Figure 8 7075: micrograph of crack path (ΔK = 8.2 MPa $\sqrt{m}$)

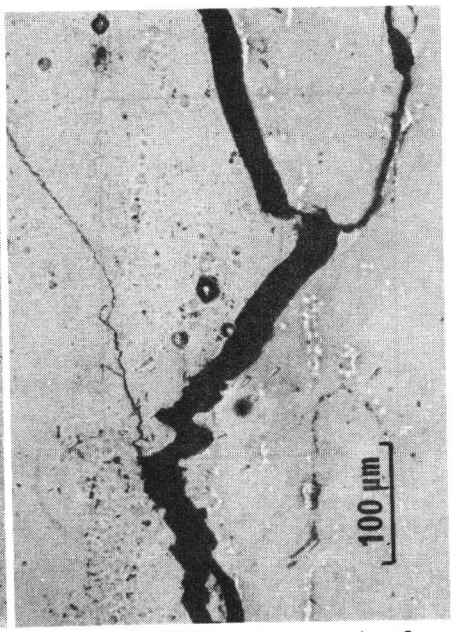

Figure 9 7X75: micrograph of crack path (ΔK = 8.5 MPa $\sqrt{m}$)

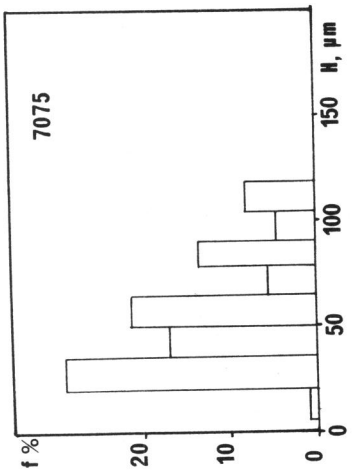

Figure 10 7075: Relative frequency of roughness heights

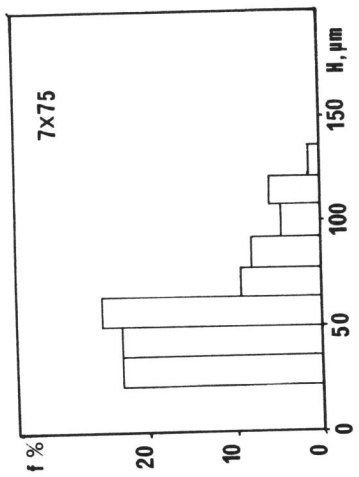

Figure 11 7X75: Relative frequency of roughness heights